VIP Cyclic Carbenes Very Important Paper

How to cite: *Angew. Chem. Int. Ed.* **2020**, *59*, 13643–13646
International Edition: doi.org/10.1002/anie.201915618
German Edition: doi.org/10.1002/ange.201915618

An Electron-Rich Cyclic (Alkyl)(Amino)Carbene on Au(111), Ag(111), and Cu(111) Surfaces

Anne Bakker[+], Matthias Freitag[+], Elena Kolodzeiski, Peter Bellotti, Alexander Timmer, Jindong Ren, Bertram Schulze Lammers, Daniel Moock, Herbert W. Roesky, Harry Mönig, Saeed Amirjalayer, Harald Fuchs, and Frank Glorius**

Dedicated to Prof. Albert Eschenmoser on the occasion of his 95th birthday

Abstract: *The structural properties and binding motif of a strongly σ-electron-donating N-heterocyclic carbene have been investigated on different transition-metal surfaces. The examined cyclic (alkyl)(amino)carbene (CAAC) was found to be mobile on surfaces, and molecular islands with short-range order could be found at high coverage. A combination of scanning tunneling microscopy (STM), X-ray photoelectron spectroscopy (XPS), and density functional theory (DFT) calculations highlights how CAACs bind to the surface, which is of tremendous importance to gain an understanding of heterogeneous catalysts bearing CAACs as ligands.*

In recent years, N-heterocyclic carbenes (NHCs) have received great attention in a broad range of applications as catalysts and as ligands for p-block elements and transition metals.[1] As a consequence of their strong σ-donating properties and their tunable side groups, NHCs are privileged ligands for NHC-metal complexes as well as the stabilization and functionalization of nanoparticles[2] and surfaces.[3] Cyclic (alkyl)(amino)carbenes (CAAC) are a prominent class of NHCs that exhibit even stronger σ-donating properties than imidazole-based NHCs.[4] Therefore, CAACs are especially valuable ligands for Rh-based hydrogenation catalysts, which can be used to hydrogenate highly functionalized (hetero)-aromatic rings with excellent functional group tolerance and conformational control.[4c,5] Moreover, they are also used as ligands for metathesis catalysts and are even able to activate small molecules such as H_2, CO, NH_3, silanes, phosphenes, and organoboron species because of their high nucleophilicity.[6] Johnson and co-workers showed that CAACs can insert into Si–H bonds on heterogeneous surfaces, and that this does not result in a binding mode comparable to a single carbene bond in CAAC-metal complexes.[7] Bullock and co-workers further studied their behavior in Rh-catalyzed hydrogenation reactions and found the protonated CAAC to coordinate exclusively to the surface.[7,8] Over the last few years, several studies of NHCs on surfaces have been reported, including STM and XPS investigations.[3b,9] The formation of ultrastable self-assembled monolayers was shown, as well as the mobility of some NHCs because of the formation of ballbot-like species and the influence of the N substituents on the binding mode to the surface.[3b,9a,b,d] However, the fundamental behavior of CAACs has been only rarely explored and there is no report of CAACs on transition-metal surfaces. Furthermore, investigations of CAACs with molecular resolution, which would be necessary to design more efficient and selective catalysts, have not been reported. Thus, we investigated the on-surface behavior of DiMeCAAC[10] (Figure 1 A), which is a rather small and structurally simple CAAC. To avoid contamination of the surface by salts and

[*] A. Bakker,[+] E. Kolodzeiski, Dr. A. Timmer, Dr. J. Ren, B. Schulze Lammers, Dr. H. Mönig, Dr. S. Amirjalayer, Prof. Dr. H. Fuchs
Physikalisches Institut
Westfälische Wilhelms-Universität
Wilhelm-Klemm-Strasse 10, 48149 Münster (Germany)
E-mail: fuchsh@uni-muenster.de

A. Bakker,[+] E. Kolodzeiski, Dr. A. Timmer, Dr. J. Ren, B. Schulze Lammers, Dr. H. Mönig, Dr. S. Amirjalayer, Prof. Dr. H. Fuchs
Center for Nanotechnology
Heisenbergstrasse 11, 48149 Münster (Germany)

Dr. M. Freitag,[+] P. Bellotti, D. Moock, Prof. Dr. F. Glorius
Organisch-Chemisches Institut
Westfälische Wilhelms-Universität
Corrensstrasse 40, 48149 Münster (Germany)
E-mail: glorius@uni-muenster.de

E. Kolodzeiski, Dr. S. Amirjalayer
Center for Multiscale Theory and Computation
Westfälische Wilhelms-Universität
Corrensstrasse 40, 48149 Münster (Germany)

Dr. A. Timmer
nanoAnalytics GmbH
Heisenbergstrasse 11, 48149 Münster (Germany)

Prof. Dr. H. W. Roesky
Institut für Anorganische Chemie
Georg-August-Universität Göttingen
Tammannstrasse 4, 37077, Göttingen (Germany)

[+] These authors contributed equally to this work.

Supporting information and the ORCID identification numbers for some of the authors of this article can be found under: https://doi.org/10.1002/anie.201915618.

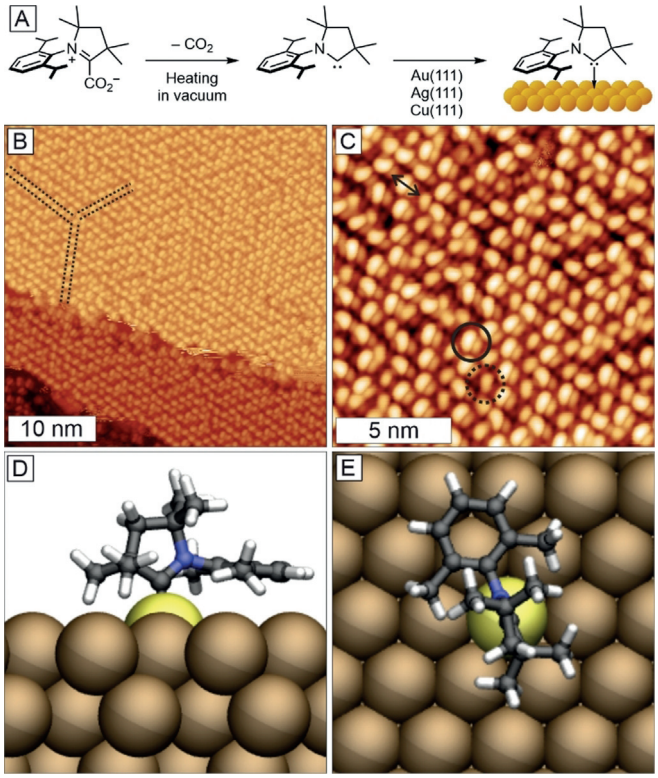

Figure 1. A) The deposition procedure for DiMeCAAC. B) Overview STM image of a full layer of DIMeCAAC on Au(111) (−2.0 V; 25 pA). C) Small-scale STM image where the individual molecular features appear as bright ellipses (methyl groups pointing upwards) and a dimmer shadow (Dipp group; −2.0 V; 25 pA). D,E) Side and top views of the DFT-optimized geometry of the upright binding mode of DiMeCAAC on Au(111).

solvent, the CO_2 adduct was used.[9a,d] DiMeCAAC·CO_2 was synthesized by the formation of the free carbene and subsequent treatment with dry CO_2, which led to precipitation of the pure material. GC-MS measurements revealed that the free CAAC can be generated without destruction.

After vacuum-depositing DiMeCAAC for 10 minutes at 60 °C on a Au(111) crystal at room temperature, an almost completely covered sample was obtained (Figure 1B). Three preferential directions of short-range order can be recognized in the molecular monolayer (Figure 1B). However, the long-range packing is not well-ordered because of the multiple different orientations adopted by the molecular features on the surface.

The same repeating shape can be recognized in the STM contrast, represented by a bright ellipse with a dimmer shadow (solid circle in Figure 1C). The distance between the different bright spots is 1.02 ± 0.09 nm. This value is the average of distances measured along all three directions, as indicated in Figure 1B with obvious defects ignored. Since DiMeCAAC forms no well-ordered self-assembled monolayer, a unit cell cannot be defined. However, the consistent value for the intermolecular distance indicates that the packing is not completely disordered.

DFT simulations predicted an upright binding mode for DiMeCAAC on Au(111) (Figure 1D) with the di-isopropylphenyl (Dipp) group perpendicular to the CAAC ring and parallel to the surface, which minimizes steric hindrance. Considering this optimized structure, the two methyl groups in the backbone point upwards and should thus give the brightest STM contrast. The bright dots in Figure 1C are, therefore, assigned to these groups. Based on these considerations, the Dipp group is attributed to the dimmer shadow. The distance between these two features (arrow in Figure 1C) is measured to be 0.44 ± 0.02 nm, which is in good agreement with the DFT-calculated distance of 0.46 nm between the upright methyl groups and the edge of the Dipp group. Not all molecular features appear equally bright (dotted circle in Figure 1C), which is attributed to a possible tilting in the adopted binding configuration (see below).

Two observations can be made when a lower coverage (ca. 80%) of DiMeCAAC is deposited on Au(111). Firstly, an adsorption preference at the elbow positions and the fcc phases of the herringbone reconstruction is observed (Figures 2A and S1), which is in agreement with the behavior of other NHCs.[9a] Secondly, the STM contrast is blurred between the islands and the visibility of the Au(111) herringbone reconstruction is reduced. This is an indication of mobility of the molecules on the surface. To illustrate this, a series of STM images was recorded on a low coverage (ca. 20%) sample (Figure 2B–D). Small molecular islands nucleate from the elbow positions of the herringbone reconstruction (Figure 2B). The shape of the islands in this image is transferred to the subsequent STM images in Figure 2C,D. Here it can be observed clearly how molecules appear and disappear, thereby changing the shape of the island between subsequent images. The adsorption energy of DiMeCAAC on Au(111) is calculated to be $E_{ads} = 2.49$ eV, which indicates a strong binding. This energy is comparable to the adsorption energy calculated previously for a mobile NHC (IPr, 2.78 eV).[9a] Here it was shown that NHCs, after binding to a gold atom, can extract this atom from the surface and thereby form a so-called ballbot species. The observed mobility of DiMeCAAC at low coverage indicates that CAACs are also capable of forming such species (Figure 2E). The adsorption energy of such a DiMeCAAC-Au ballbot-like species was calculated to be 4.11 eV, which is significantly higher than the adsorption energy of the surface-bound species. Furthermore, the mobility of such a DiMeCAAC-Au species was investigated by DFT calculations. The differences in the binding energy along the lateral diffusion pathway were found to be smaller than 0.04 eV (see the Supporting Information), which indicates low diffusion barriers.

The preferred adsorption position of a DiMeCAAC-Au species is calculated to be at the hollow site of the Au(111) surface (see the Supporting Information). Based on this, a possible, theoretical close-packed self-assembled structure was calculated (Figure 2F). The distance between the adatoms in this image is 0.89 nm, which is smaller than the experimentally determined average value of 1.02 ± 0.09 nm. This shows that DiMeCAAC can not easily assemble in a well-ordered, close-packed self-assembled monolayer, as the STM images clearly indicate (Figure 1B). In principle, the atomic lattice of the surface is driving the organization of the DiMeCAAC-Au species on the surface by the preferred

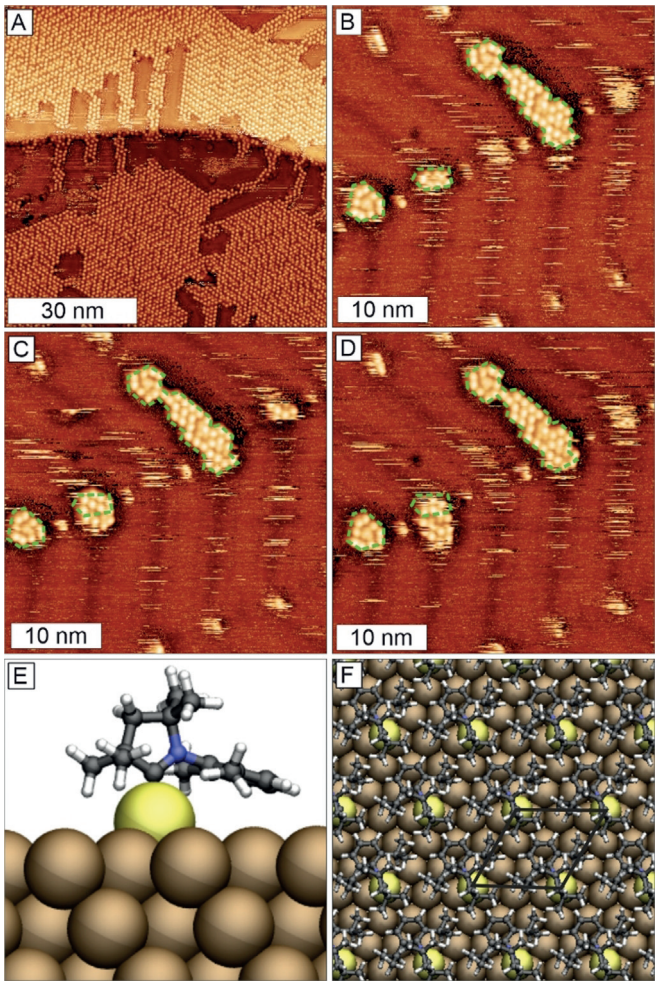

Figure 2. A) Overview STM image of DiMeCAAC on Au(111) at ca. 80% coverage showing a preferred adsorption at the fcc phase of the herringbone reconstruction (−2.0 V; 16 pA). B–D) Subsequent STM images of the same area of a low coverage (ca. 20%) sample showing a change in the size of the molecular islands as a result of the appearance and disappearance of molecules (−2.0 V; 17 pA). E) DFT-optimized geometry of a DiMeCAAC-Au ballbot species on the surface. F) A theoretical close-packed self-assembly of DiMeCAAC-Au ballbot-like species on Au(111).

adsorption at the hollow sites. Since the main interaction of these species with the surface is through the gold atom, molecules can arrive with any orientation at an island of molecules. However, as a consequence of the bulky Dipp group and the asymmetric structure of the molecule, intermolecular interactions are possible and rotation of individual ballbots in a molecular island is limited. Combined with the mobility of the molecules and the required high coverage for STM imaging, this makes it more difficult to reach the optimized self-assembled structure. However, by positioning the atomic lattice over the STM images, preferred adsorption at or very close to the hollow site can be observed for most of the molecules (see the Supporting Information). Attempts to deposit more slowly (70 min at 45 °C) did not result in an improved order in the molecular layer. Annealing of the sample after deposition could also not induce a more ordered structure, but instead led to desorption of the molecules. In addition, the calculated DiMeCAAC-Au configuration (Figure 2E) allows for a slight tilting to the sides when the distance to neighboring molecules is larger. This explains the differences in the brightness observed in Figure 1C. DiMeCAAC was also investigated on Ag(111) and Cu(111), which gave similar results as on Au(111), as can be seen from the STM images in the Supporting Information.

To confirm the intact deposition of DiMeCAAC and to obtain more chemical information about the species on the surface, GC-MS measurements of DiMeCAAC·CO_2 and XPS measurements of DiMeCAAC on Au(111) were performed. A requirement for GC-MS analysis is the intact evaporation of the molecule. At inlet temperatures of more than 200 °C, the molecule decarboxylates as expected and releases the free CAAC, which resulted in a single peak with the parent ion signal at $m/z = 285.30$ (see the Supporting Information). This is in agreement with the mass of the free CAAC within the error of the quadrupole mass analyzer used. Since DiMeCAAC only has one nitrogen atom, we used N 1s XPS analysis as a marker to investigate the intact nature of the DiMeCAAC on the surface. The resulting XPS spectrum is plotted in Figure 3A. A clear single peak is observed at 400.7 eV, as expected for deposition of intact molecules. XPS literature for CAACs bound to transition metals is not available. However, N 1s binding energies around 400 to 401 eV are typically reported for NHCs bound to Au(111) surfaces or nanoparticles.[3b,9d,e,11] We, therefore, conclude that the peak at 400.7 eV corresponds to surface-bound CAAC molecules. In addition, the O 1s XPS spectrum shows negligible traces of oxygen on the surface, thus confirming the removal of CO_2 during sample preparation.

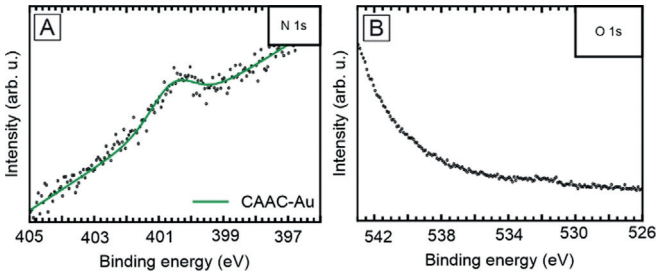

Figure 3. A) N 1s XPS spectrum of a monolayer of DiMeCAAC on Au(111) with a peak at 400.7 eV. The corresponding STM image can be found in Figure 1B. B) O 1s XPS spectrum of the same sample showing a negligible trace of oxygen on the surface, thus confirming the removal of CO_2 during sample preparation.

In summary we have shown the successful deposition of DiMeCAAC on different transition-metal surfaces by evaporation of the CO_2 adduct in ultrahigh vacuum. Molecular islands with short-range order were found; however, the unsymmetric nature and bulky side group of the molecule means that a well-ordered, close-packed self-assembled structure cannot be obtained. At lower coverage, preferred adsorption at the fcc phase of the herringbone reconstruction was observed. Furthermore, a series of STM images showed that DiMeCAAC is mobile on the surface, which can be explained by the formation of ballbot-like species, as

observed previously for other NHCs. Furthermore, the intact deposition of DiMeCAAC was confirmed by a single peak in the N 1s XPS spectrum and the removal of the CO_2 groups was confirmed by the O 1s XPS spectrum. This investigation of a CAAC on different surfaces opens the way for further studies on more complex (chiral, functional) CAAC ligands.

Acknowledgements

This work was generously supported by the Deutsche Forschungsgemeinschaft through the collaborative research center SFB 858 (project B03), and through projects AM 460/2-1, MO 2345/4-1 and FU 299/19. Furthermore, we thank nanoAnalytics GmbH for technical support.

Conflict of interest

The authors declare no conflict of interest.

Keywords: CAAC · gold surfaces · ligands · scanning probe microscopy · X-ray photoelectron spectroscopy

[1] a) M. N. Hopkinson, C. Richter, M. Schedler, F. Glorius, *Nature* **2014**, *510*, 485 – 496; b) A. V. Zhukhovitskiy, M. J. MacLeod, J. A. Johnson, *Chem. Rev.* **2015**, *115*, 11503 – 11532; c) C. A. Smith, M. R. Narouz, P. A. Lummis, I. Singh, A. Nazemi, C.-H. Li, C. M. Crudden, *Chem. Rev.* **2019**, *119*, 4986 – 5056.

[2] a) L. S. Ott, M. L. Cline, M. Deetlefs, K. R. Seddon, R. G. Finke, *J. Am. Chem. Soc.* **2005**, *127*, 5758 – 5759; b) E. C. Hurst, K. Wilson, I. J. S. Fairlamb, V. Chechik, *New J. Chem.* **2009**, *33*, 1837; c) J. Vignolle, T. D. Tilley, *Chem. Commun.* **2009**, 7230 – 7232; d) K. V. S. Ranganath, J. Kloesges, A. H. Schäfer, F. Glorius, *Angew. Chem. Int. Ed.* **2010**, *49*, 7786 – 7789; *Angew. Chem.* **2010**, *122*, 7952 – 7956; e) E. A. Baquero, S. Tricard, J. C. Flores, E. de Jesús, B. Chaudret, *Angew. Chem. Int. Ed.* **2014**, *53*, 13220 – 13224; *Angew. Chem.* **2014**, *126*, 13436 – 13440; f) M. J. MacLeod, J. A. Johnson, *J. Am. Chem. Soc.* **2015**, *137*, 7974 – 7977; g) J. B. Ernst, S. Muratsugu, F. Wang, M. Tada, F. Glorius, *J. Am. Chem. Soc.* **2016**, *138*, 10718 – 10721; h) C.-Y. Wu, W. J. Wolf, Y. Levartovsky, H. A. Bechtel, M. C. Martin, F. D. Toste, E. Gross, *Nature* **2017**, *541*, 511 – 515; i) J. B. Ernst, C. Schwermann, G.-I. Yokota, M. Tada, S. Muratsugu, N. L. Doltsinis, F. Glorius, *J. Am. Chem. Soc.* **2017**, *139*, 9144 – 9147; j) R. W. Y. Man, C.-H. Li, M. W. A. MacLean, O. V. Zenkina, M. T. Zamora, L. N. Saunders, A. Rousina-Webb, M. Nambo, C. M. Crudden, *J. Am. Chem. Soc.* **2018**, *140*, 1576 – 1579; k) M. R. Narouz, K. M. Osten, P. J. Unsworth, R. W. Y. Man, K. Salorinne, S. Takano, R. Tomihara, S. Kaappa, S. Malola, C.-T. Dinh, J. D. Padmos, K. Ayoo, P. J. Garrett, M. Nambo, J. H. Horton, E. H. Sargent, H. Häkkinen, T. Tsukuda, C. M. Crudden, *Nat. Chem.* **2019**, *11*, 419 – 425.

[3] a) A. V. Zhukhovitskiy, M. G. Mavros, T. van Voorhis, J. A. Johnson, *J. Am. Chem. Soc.* **2013**, *135*, 7418 – 7421; b) C. M. Crudden, J. H. Horton, I. I. Ebralidze, O. V. Zenkina, A. B. McLean, B. Drevniok, Z. She, H.-B. Kraatz, N. J. Mosey, T. Seki, E. C. Keske, J. D. Leake, A. Rousina-Webb, G. Wu, *Nat. Chem.* **2014**, *6*, 409 – 414; c) A. Lv, M. Freitag, K. M. Chepiga, A. H. Schäfer, F. Glorius, L. Chi, *Angew. Chem. Int. Ed.* **2018**, *57*, 4792 – 4796; *Angew. Chem.* **2018**, *130*, 4883 – 4887; d) E. A. Doud, M. S. Inkpen, G. Lovat, E. Montes, D. W. Paley, M. L. Steigerwald, H. Vázquez, L. Venkataraman, X. Roy, *J. Am. Chem. Soc.* **2018**, *140*, 8944 – 8949; e) R. Ye, A. V. Zhukhovitskiy, R. V. Kazantsev, S. C. Fakra, B. B. Wickemeyer, F. D. Toste, G. A. Somorjai, *J. Am. Chem. Soc.* **2018**, *140*, 4144 – 4149; f) D. T. Nguyen, M. Freitag, M. Körsgen, S. Lamping, A. Rühling, A. H. Schäfer, M. H. Siekman, H. F. Arlinghaus, W. G. van der Wiel, F. Glorius, B. J. Ravoo, *Angew. Chem. Int. Ed.* **2018**, *57*, 11465 – 11469; *Angew. Chem.* **2018**, *130*, 11637 – 11641.

[4] a) V. Lavallo, Y. Canac, C. Präsang, B. Donnadieu, G. Bertrand, *Angew. Chem. Int. Ed.* **2005**, *44*, 5705 – 5709; *Angew. Chem.* **2005**, *117*, 5851 – 5855; b) M. Soleilhavoup, G. Bertrand, *Acc. Chem. Res.* **2015**, *48*, 256 – 266; c) M. Melaimi, R. Jazzar, M. Soleilhavoup, G. Bertrand, *Angew. Chem. Int. Ed.* **2017**, *56*, 10046 – 10068; *Angew. Chem.* **2017**, *129*, 10180 – 10203.

[5] M. P. Wiesenfeldt, Z. Nairoukh, W. Li, F. Glorius, *Science* **2017**, *357*, 908 – 912.

[6] D. A. Ruiz, G. Ung, M. Melaimi, G. Bertrand, *Angew. Chem. Int. Ed.* **2013**, *52*, 7590 – 7592; *Angew. Chem.* **2013**, *125*, 7739 – 7742.

[7] A. V. Zhukhovitskiy, M. G. Mavros, K. T. Queeney, T. Wu, T. van Voorhis, J. A. Johnson, *J. Am. Chem. Soc.* **2016**, *138*, 8639 – 8652.

[8] a) B. L. Tran, J. L. Fulton, J. C. Linehan, J. A. Lercher, R. M. Bullock, *ACS Catal.* **2018**, *8*, 8441 – 8449; b) B. L. Tran, J. L. Fulton, J. C. Linehan, M. Balasubramanian, J. A. Lercher, R. M. Bullock, *ACS Catal.* **2019**, *9*, 4106 – 4114.

[9] a) G. Wang, A. Rühling, S. Amirjalayer, M. Knor, J. B. Ernst, C. Richter, H.-J. Gao, A. Timmer, H.-Y. Gao, N. L. Doltsinis, F. Glorius, H. Fuchs, *Nat. Chem.* **2017**, *9*, 152 – 156; b) C. R. Larrea, C. J. Baddeley, M. R. Narouz, N. J. Mosey, J. H. Horton, C. M. Crudden, *ChemPhysChem* **2017**, *18*, 3536 – 3539; c) L. Jiang, B. Zhang, G. Medard, A. P. Seitsonen, F. Haag, F. Allegretti, J. Reichert, B. Kuster, J. V. Barth, A. C. Papageorgiou, *Chem. Sci.* **2017**, *8*, 8301 – 8308; d) A. Bakker, A. Timmer, E. Kolodzeiski, M. Freitag, H. Y. Gao, H. Mönig, S. Amirjalayer, F. Glorius, H. Fuchs, *J. Am. Chem. Soc.* **2018**, *140*, 11889 – 11892; e) G. Lovat, E. A. Doud, D. Lu, G. Kladnik, M. S. Inkpen, M. L. Steigerwald, D. Cvetko, M. S. Hybertsen, A. Morgante, X. Roy, L. Venkataraman, *Chem. Sci.* **2019**, *10*, 930 – 935.

[10] A. P. Singh, P. P. Samuel, H. W. Roesky, M. C. Schwarzer, G. Frenking, N. S. Sidhu, B. Dittrich, *J. Am. Chem. Soc.* **2013**, *135*, 7324 – 7329.

[11] a) A. Rühling, K. Schaepe, L. Rakers, B. Vonhören, P. Tegeder, B. J. Ravoo, F. Glorius, *Angew. Chem. Int. Ed.* **2016**, *55*, 5856 – 5860; *Angew. Chem.* **2016**, *128*, 5950 – 5955; b) M. R. Narouz, C.-H. Li, A. Nazemi, C. M. Crudden, *Langmuir* **2017**, *33*, 14211 – 14219; c) A. J. Young, M. Sauer, G. M. D. M. Rubio, A. Sato, A. Foelske, C. J. Serpell, J. M. Chin, M. R. Reithofer, *Nanoscale* **2019**, *11*, 8327 – 8333.

Manuscript received: December 6, 2019
Revised manuscript received: April 7, 2020
Accepted manuscript online: April 8, 2020
Version of record online: June 3, 2020

